

# Rheology and Shear Band Suppression in Particle and Chain Mixtures

I. Regev and C. Reichardt

*Center for Nonlinear Studies and Theoretical Division,  
Los Alamos National Laboratory, Los Alamos, New Mexico 87545*

(Dated: July 6, 2018)

Using numerical simulations, we consider an amorphous particle mixture which exhibits shear banding, and find that the addition of even a small fraction of chains strongly enhances the material strength, creating pronounced overshoot features in the stress-strain curves. The strengthening occurs in the case where the chains are initially perpendicular to the shear direction, leading to a suppression of the shear band. For large strain, the chains migrate to the region where a shear band forms, resulting in a stress drop. The alignment of the chains by the shear bands results in a Bauschinger-like effect for subsequent reversed shear. Many of these features are captured in a simple model of a single chain being pulled through a viscous material. Our results are also useful for providing insights into methods of controlling and strengthening granular materials against failure.

PACS numbers:

Sheared amorphous jammed materials such as colloids, foams, and granular media can exhibit a rich variety of dynamics, such as strain localization (shear bands) [1–5], nonequilibrium phases [6], and dynamic ordering [7]. Most studies of these systems are performed with spherical or elliptical particles; however, recent work has explored the packing or shearing of chains or granular polymer systems [8, 9]. Jamming and packing studies of granular chains indicate that as the chain length increases, the jamming density falls further below the jamming density of monomer assemblies [8, 10]. In shear-strain experiments with three-dimensional (3D) granular chain packings, a strain stiffening behavior has been observed [9] that resembles the behavior found in some polymer systems [11, 12]. The granular chain experiments also revealed a maximum in the stress as a function of strain that corresponds to the point at which the chains begin to break. These results suggest that the addition of chains to monomer packings could significantly alter the viscoplastic response, and that granular materials could be strengthened by the addition of flexible chains of some form. Understanding the effect of adding chains to a granular material could also have significant practical applications for preventing failures of granular piles or avalanches and for developing methods to suppress shear band formation in materials.

Here we examine the stress-strain relations for an amorphous packing of particles that exhibits shear banding in the absence of chains. With the addition of even a small fraction of granular chains, the system sustains remarkably higher amounts of stress and exhibits a stress-strain overshoot. The maximum stress at the peak of the overshoot increases with increasing chain length. The strengthening effect depends on the initial orientation of the chains with respect to the shear direction, with the maximum effect occurring when the chains are initially perpendicular to the shear. The effect arises due to the suppression by the chains of the formation of a shear band in the monomer component of the material. Un-

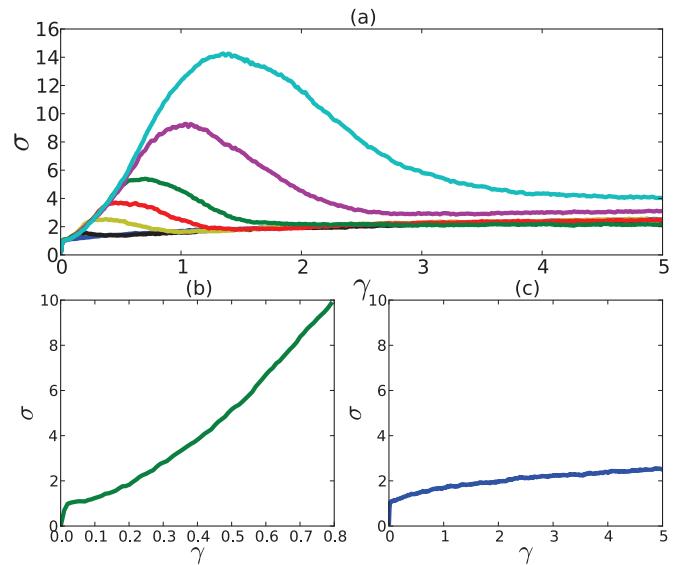


FIG. 1: (Color online) (a) The stress-strain curves  $\sigma$  vs  $\gamma$  for an amorphous solid system with a chain added perpendicular to the shear direction. From bottom to top, chain length  $L = 0$  (no chain),  $W/4$ ,  $W/2$ ,  $3W/4$ ,  $W$ ,  $3W/2$ , and  $2W$ , where  $W = \sqrt{N}$ . Here  $\dot{\gamma} = 5 \cdot 10^{-2}$ , and the chain-free system exhibits shear banding. A stress overshoot phenomenon develops as the chain length increases. For  $L = 2W$ , the fraction of particles in the chain is  $N_c/N = 0.03125$ . (b) A blowup of the  $L = 2W$  curve from (a) showing strain stiffening. (c) A blowup of the chain-free system in (a) where strain stiffening is absent.

der increasing strain, the chains gradually migrate into the regions that are prone to shear band formation, leading to the stress decrease and the development of shear bands. After the peak in the stress overshoot, the stress returns to the value found for a system containing only monomers. The shear-induced alignment of the chains also leads to a behavior that resembles the Bauschinger effect as the strain is cycled. We show that many of the

features of the system can be captured by a simple model of a chain immersed in a viscous fluid and pulled at one end.

*Simulation*— We consider a system of  $N$  particles with pairwise harmonic force interactions  $\mathbf{F}_{dd}^i = \sum_{j \neq i}^N k_g (r_{\text{eff}}^{ij} - R_{ij}) \Theta(r_{\text{eff}}^{ij} - R_{ij}) \hat{\mathbf{R}}_{ij}$  with a spring constant of  $k_g = 300$ , where  $\mathbf{R}_{i(j)}$  is the position of particle  $i(j)$ ,  $R_{ij} = |\mathbf{R}_i - \mathbf{R}_j|$ ,  $\hat{\mathbf{R}}_{ij} = (\mathbf{R}_i - \mathbf{R}_j)/R_{ij}$ ,  $\Theta$  is the Heaviside step function,  $r_{\text{eff}}^{ij} = r_i + r_j$ , and  $r_{i(j)}$  is the radius of disk  $i(j)$ . To ensure that the disk packings are amorphous, we use a binary distribution of disks where we set half the disk radii to  $r_i = 1.0$  and the other half to  $r_i = 1.4$ . The chains are modeled as connected disks that have the same harmonic interactions with the surrounding disks and experience an additional force  $F_c^i = \sum_k k_c k_g (r_{\text{eff}}^{ik} - R_{ik}) \hat{\mathbf{R}}_{ik}$  where the disks  $k$  are the immediate neighbors of the disk  $i$  along the chain. Here  $k_c$  is the spring constant of the chain interaction, and a given chain contains  $N_c$  particles. We use an overdamped equation of motion which gives athermal dissipative dynamics,  $m_i \dot{\mathbf{p}}_i = \mathbf{F}^i - \eta \mathbf{v}_i$ , with  $\mathbf{F}^i = \mathbf{F}_{dd}^i + \mathbf{F}_c^i$ . Here the damping coefficient  $\eta = 10$  and the masses of the disks are set to  $m_i = 1.0$ . The equations of motion are solved using the Leap-Frog algorithm. To initialize the system, we place one or more chains in a region of the plane, and randomly distribute other monomers around it. We then compress the system to a density  $\phi = 1.1624$ ; this is well into the jammed state, as the jamming density for this system has been shown to occur at  $\phi_j \approx 0.844$  [15, 16, 21, 22]. Shear is induced via the Lees-Edwards boundary conditions [20]. These boundary conditions have previously been employed for the chain-free version of this system near jamming [15, 16]. Similar boundary conditions have been employed in experiments studying shear-bands [17, 18].

*Results*— In the absence of a chain, the monomer system exhibits a shear banding effect when  $\dot{\gamma}$  is sufficiently large. Figure 1(a) shows the stress-strain  $\sigma - \gamma$  curves for a system with  $N = 4096$  disks with  $\dot{\gamma} = 5 \cdot 10^{-2}$ , which is large enough for shear banding to occur in the chain-free system. For a chain-free sample, there is a linear elastic regime followed by yield and a plastic regime where a shear band forms, as illustrated in Fig. 1(c). At higher  $\dot{\gamma}$ ,  $\sigma$  is roughly constant with a value near  $\sigma = 2.0$ . When a chain of length  $L$  is placed in the system perpendicular to the shear direction, we observe the development of a stress overshoot that becomes larger as  $L$  increases. This is shown in Fig. 1(a) for chains of length ranging from  $L = W/4$  to  $L = 2W$ , where  $W = \sqrt{N}$  is the width of the system. For the longest chain  $L = 2W$ , which contains a fraction of only  $N_c/N = 0.03125$  (about 3%) of the total number of grains in the system, the peak value of  $\sigma$  is almost ten times higher than for the chain-free system. In Fig. 1(b), a blowup of the  $\sigma - \gamma$  curve for the  $L = 2W$  system illustrates a strain stiffening response, indicated by  $\sigma$  growing nonlinearly with  $\gamma$ . The initial

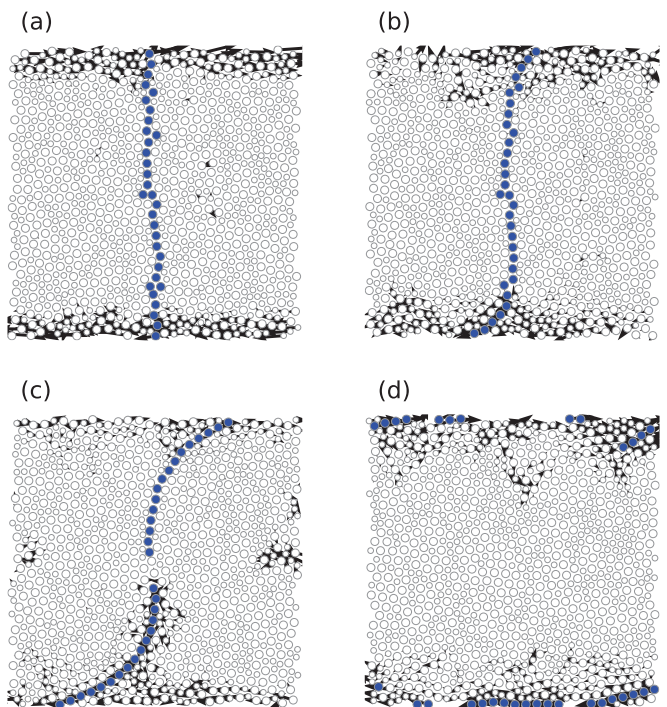


FIG. 2: (Color online) Particle locations (open circles), chain location (filled circles), and motion (arrows) for the system in Fig. 1 with chain length  $L = W$ . (a) The initial state at  $\gamma = 0.013$  where the chain is aligned perpendicular to the shear direction. (b)  $\gamma = 0.25$ . (c)  $\gamma = 0.625$ , close to the peak of the stress. (d)  $\gamma = 2.0$ , after the stress drop (for a more vivid visualization see also animation in supplementary material).

increase of  $\sigma$  can be fit approximately to  $\sigma \propto \gamma^2$ . Figure 1(c) shows the chain-free system where strain stiffening is absent (the system actually experiences mild strain-softening). These results are similar to those observed in experimental studies of 3D systems of pure chains, where a strain stiffening response is most pronounced for longer chains that also have a peak in the stress-strain curves [9]. The strain stiffening was attributed in [9] to entanglements, which do not occur in our system due to the diluteness of our chains and the two-dimensional (2D) nature of our system. Additionally, in the experimental system, the drop in the stress above the peak response is due to the chains breaking, something that is not permitted to occur in our system.

A better understanding of the  $\sigma - \gamma$  overshoot is provided by the images in Fig. 2 of a chain with  $L = W$  immersed in a smaller system  $N = 1024$ . In Fig. 2(a), taken at the very small strain of  $\gamma = 0.013$ , the initial placement of the chain perpendicular to the shear direction is barely disturbed. As  $\gamma$  increases to  $\gamma = 0.25$ , shown in Fig. 2(b), the chains begin to stretch and form an S shape at the top and bottom of the sample where the shear band forms in the absence of a chain. Figure

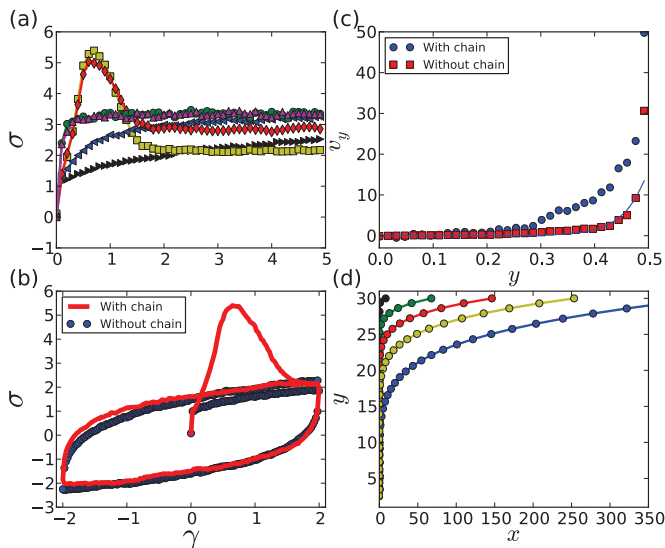


FIG. 3: (Color online) (a) The effect of strain rate on the  $\sigma$ - $\gamma$  curves for  $\dot{\gamma} = 10^{-3}$ ,  $10^{-2}$ , and  $5 \times 10^{-2}$  for the chain-free (green circles, blue left-triangles and black-right triangles respectively) and  $L = W$  (magenta up-triangles, red diamonds and yellow squares respectively) samples. At  $\dot{\gamma} = 10^{-3}$  in the sample containing a chain, there is no shear band formation and the overshoot phenomenon is absent. (b)  $\sigma$ - $\gamma$  curves for the system in Fig. 1 with  $L = W$  (thin red curve) and with no chain (blue circles) obtained for cyclic applied strain. Here the stress overshoot only occurs during the initial strain increase in the presence of the chain, and the chain remains inside the shear band during subsequent strain cycles. (c) Velocity profile of the particles near the moving boundary at  $\gamma = 0.05$ . The red squares are the curve for the system with no chain that show the usual exponential decay (solid blue line is an exponential fit) as expected [1, 4]. The blue circles are the curve for the system with a chain that does not fit an exponential profile. (d) Chain configuration at different times for a simple model of a chain with  $k_c = 0.3$  in a viscous media pulled by the top bead with constant  $v_x$ . Time increases from the left-most (black) curve to the right-most (blue) curve.

2(c) shows that at  $\gamma = 0.625$ , where the peak value of  $\sigma$  occurs, the chain has become fully stretched and is beginning to migrate into the shear band region, while at  $\gamma = 2.0$  beyond the peak stress, Fig. 2(d) indicates that the chain has fully migrated into the shear band region and that the shear band is fully formed. The peak in  $\sigma$  occurs due to the suppression of the shear band in the monomers by the creation by the chain of an effective coupling between the particles in the shear band region and the particles in the bulk region at the center of the sample. The shear band develops rapidly once the chain aligns with the shear direction, leading to the stress drop. A further indication that the realignment of the chain with the shear band is responsible for the stress drop appears in Fig. 3(b), where we plot the  $\sigma$ - $\gamma$  curve for the  $L = W$  sample under cyclic applied strain.

As was mentioned above, the hardening effect appears

to be related to the suppression of shear-bands. Since shear bands in granular matter appear for high strain rates (see, for example, [19]), changing the strain rate  $\dot{\gamma}$  should alter the hardening behavior. In Fig. 3(a) we plot the  $\sigma$ - $\gamma$  curves for a chain-free system at  $\dot{\gamma} = 10^{-3}$ ,  $10^{-2}$  and  $5 \times 10^{-2}$  along with the corresponding curves in the presence of an  $L = W$  chain. In the chain-free system, the steady state value of  $\sigma$  for  $\dot{\gamma} = 10^{-3}$  where shear banding does not occur is higher than for samples with higher  $\dot{\gamma}$  where shear banding takes place. When an  $L = W$  chain is added to the system, at  $\dot{\gamma} = 10^{-3}$  the  $\sigma$ - $\gamma$  curve is almost identical to that found for the chain-free case. Although the chain still gradually aligns with the shear direction, there is no shear band to block at this strain rate, and thus no difference in response when the chain is added. The hardening and stress overshoot due to the presence of a chain appears only at rates high enough for shear band formation, shown in Fig. 3(a). At large strains, the samples containing a chain have a lower value of  $\sigma$  than the chain-free systems subjected to the same strain and strain rate. This is due to a lubrication effect which also seems to be important only at higher strain-rates. This indicates that in some cases the addition of a chain can decrease rather than increasing the stress.

An overshoot only occurs during the initial increase in the strain when the chain has not yet aligned with the shear band. Once the chain has entered the shear band region, it remains there even when the strain rate is reversed, and subsequent cycles of the strain produce stress curves that closely follow those obtained for a system without chains, as shown in Fig. 3(b). The change in the  $\sigma$ - $\gamma$  curves upon reversing the strain resembles the Bauschinger effect - the material responds differently to positive or negative shear on the same axis - which occurs in amorphous solids and crystals. In the chain system this effect vanishes after the first shearing cycle. In Fig. 3(c) we can observe the difference in the velocity profile between the chain-free and chain configurations. The chain-free configuration shows the typical exponential behavior (see [1, 4]) while the chain configuration shows a more gradual velocity profile.

To examine the effects of the chain stiffness, in Fig. 4(a) we plot the  $\sigma$ - $\gamma$  curves for a sample containing a chain with  $L = W$  at  $\dot{\gamma} = 5 \times 10^{-2}$  for  $k_c = 2.5, 5, 10,$  and  $20$ . The stress peak increases with decreasing  $k_c$  and the position of the peak shifts to higher strain. Figure 4(b) shows the fraction  $f_{\text{perp}}$  of the chain length oriented in the direction perpendicular to the strain versus  $\gamma$ . The chain transitions from being aligned completely perpendicularly to the strain ( $f_{\text{perp}} = 1$ ) to being aligned with the shear direction ( $f_{\text{perp}} = 0$ ). The softer chain is more difficult to pull through the bulk due to its greater tendency to meander as it interacts with the monomers. We have also tested multiple chains in the same system and found an additive effect where  $\sigma$  in a sample containing



two  $L = W$  chains is twice as large as  $\sigma$  in a sample containing only one  $L = W$  chain.

For very long chains, we observe the same general behaviors described above; however, additional nonlinear rheological effects can arise that we will describe in greater detail in another paper. Many of the features we observe in the simulation can be captured by a simple model of a single chain pulled at one end through a viscous medium. The model consists of  $L$  point particles with mass  $m = 1$  connected by springs with constant spring force  $k_c$  and a rest length  $r_0 = 1$ . Each particle experiences a drag force  $f_{drag}^i$  that is assumed to depend on the vertical distance  $\delta y$  between the particle and its lower neighbor as well as on the horizontal velocity of the particle:  $f_{drag}^i \propto \delta y_{i,i-1} v_x^i$ . The particles also experience a uniform damping force  $f_{damp} = \eta v_i$ . We fix the top of the chain to be at a constant height  $y = W$  and to move at constant velocity  $v_x$ . This represents the case where the top of the chain is dragged by a shear band and pulled at a fixed rate. In Fig. 3(d) we plot the chain configurations from this model at different times, showing that the chain gradually moves to flow behind the driven bead in a manner similar to that observed in our simulations in Fig. 2. In Fig. 4(c) we plot  $F_{tot}$  versus time for chains of length  $L = 30$  and increasing  $k_c$ . The peak value of  $F_{tot}$  increases with decreasing  $k_c$ , similar to the behavior found in our simulation. Fig. 4(d) shows the total force  $F_{tot}$  exerted on the chain by the driven bead versus time for increasing chain length  $L$ . A peak in  $F_{tot}$  occurs and is followed by a drop off, with the peak shifting to later strains and increasing in height as  $L$  increases. There are several differences between the model and the simulation, including the fact that the strain stiffening effect does not appear in the model when the strain is initially increased, and the magnitude of the peak in  $F_{tot}$  does not increase as rapidly with  $L$  in the model as does the peak in  $\sigma$  in the simulation. The model does, however, capture most features of the shapes of the curves and the behavior of the chain.

In summary, we have shown that the addition of a small fraction of chains to an amorphous solid can strongly alter the stress-strain response and can significantly strengthen the material, producing a pronounced overshoot in the stress-strain curve. This effect occurs for strain rates at which the chain-free system exhibits shear banding. When the chains are initially oriented perpendicular to the strain direction, the shear banding is partially suppressed until the chain becomes aligned with the shear direction and absorbed into the shear band, leading to a stress drop. The alignment of the chains into the shear band also produces a Bauschinger like effect for cyclic strains. For long chains we also observe a strain stiffening effect that is absent in the chain-free samples. Our results have several similarities to recent experiments in 3D systems of pure granular chains, including strain stiffening and stress overshoots; however, there are signif-

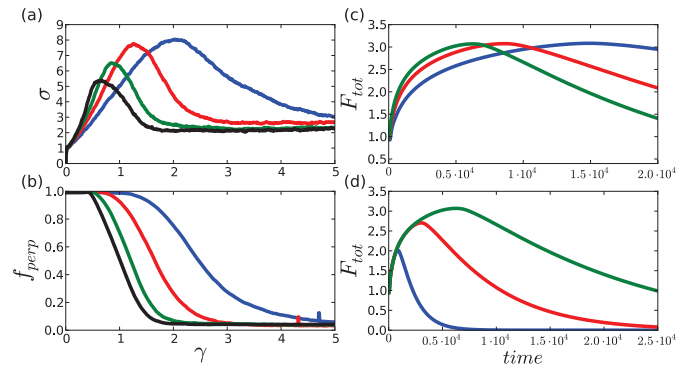


FIG. 4: (Color online) (a)  $\sigma - \gamma$  curves for the system in Fig. 1 with  $L = W$  and  $\dot{\gamma} = 5 \times 10^{-3}$  for varied chain spring constant  $k_c = 2.5, 5, 20$  and  $20$  where weaker chains produce larger but less stiff peaks. (b) The corresponding fraction  $f_{perp}$  of the chain oriented in the direction perpendicular to the strain. This figure shows that the softer chains generate a higher stress peak due to spending more time in the bulk before being pulled to the shear-band. (c) The total force  $F_{tot}$  applied to the chain in the simple model vs time for  $L = 30$  with  $k_c = 0.3, 0.2$ , and  $0.1$ , from left to right, showing the increase in stress with decreasing  $k_c$ . (d)  $F_{tot}$  vs time in the simple model for increasing chain length  $L$  showing an overshoot and an increase in the  $F_{tot}$  for longer chains. From left to right,  $L = 10, 20, 30$ . Here  $k_c = 0.3$ .

icant differences, including the fact that the stress drop after the overshoot arises due to chain alignment rather than chain breaking, and the fact that there are no entanglements in our system. Our results suggest that the response of granular media can be significantly altered and the media strengthened by the addition of even a small number of chain like particles. This could have applications for preventing failures of granular heaps and soils or preventing erosion and is another example of the importance of structure to the rheology of amorphous materials [13, 14].

The authors thank Lena Lopatina for useful discussions and Cynthia Reichhardt for carefully reviewing the manuscript. This work was carried out under the auspices of the NNSA of the U.S. DoE at LANL under Contract No. DE-AC52-06NA25396.

- 
- [1] P. Schall and M. van Hecke, *Ann. Rev. Fluid Mech.* **42**, 67 (2010).
  - [2] M.L. Falk and J.S. Langer, *Ann. Rev. Condens. Matter Phys.* **2**, 353 (2011).
  - [3] Y. Wang, K. Krishan, and M. Dennin, *Phys. Rev. E* **73**, 031401 (2006); E. Janiaud, D. Weaire and S. Hutzler, *Phys. Rev. Lett.* **97**, 038302 (2006).
  - [4] G. Katgert, M.E. Möbius, and M. van Hecke, *Phys. Rev. Lett.* **101**, 058301 (2008).
  - [5] M. L. Manning, J. S. Langer, and J. M. Carlson, *Phys. Rev. E* **76**, 056106 (2007); M.L. Manning, E.G. Daub,

- J.S. Langer, J.M. Carlson, Phys. Rev. E **79**, 016110 (2009). JJ Lewandowski and AL Greer, Nature Materials, **5** 15 (2006).
- [6] H. Katsuragi, A.R. Abate, and D.J. Durian, Soft Matter **6**, 3023 (2010); K.A. Lorincz and P. Schall, Soft Matter **6**, 3044 (2010); D. Bi, J. Zhang, B. Chakraborty, and R.P. Behringer, Nature **480**, 355 (2011).
- [7] I. Cohen, T.G. Mason, and D.A. Weitz, Phys. Rev. Lett. **93**, 046001 (2004); K.E. Daniels and R.P. Behringer, Phys. Rev. Lett. **94**, 168001 (2005); R. Besseling, E.R. Weeks, A.B. Schofield and W.C.K. Poon, Phys. Rev. Lett. **99**, 028301 (2007); D.S. Grebenkov, M.P. Ciamarra, M. Nicodemi, and A. Coniglio, Phys. Rev. Lett. **100**, 078001 (2008); Y.L. Wua, D. Derks, A. van Blaaderen, and A. Imhof, Proc. Natl. Acad. Sci. (USA) **106**, 10564 (2009).
- [8] L.-N Zou, X. Cheng, M.L. Rivers, H.M. Jaeger, and S.R. Nagel, Science **326**, 408 (2009); C.J. Olson Reichhardt and L.M. Lopatina, Science **326**, 374 (2009).
- [9] E. Brown, A. Nasto, A.G. Athanassiadis, and H.M. Jaeger, Phys. Rev. Lett. **108**, 108302 (2012).
- [10] L.M. Lopatina, C.J. Olson Reichhardt, and C. Reichhardt, Phys. Rev. E **84**, 011303 (2011).
- [11] R.S. Hoy and C.S. O'Hern, Soft Matter **8**, 1215 (2012).
- [12] C.P. Buckley and D.C. Jones, Polymer **36**, 3301 (1995).
- [13] L Boué, H. G. E. Hentschel, I. Procaccia, I. Regev, and J. Zylberg, Phys. Rev. B **81**, 100201(R) (2010).
- [14] M.L. Falk, J.S. Langer, Phys. Rev. E **57**, 71927205 (1998)
- [15] P. Olsson and S. Teitel, Phys. Rev. Lett. **99**, 178001 (2007); P. Olsson and S. Teitel, Phys. Rev. E **83**, 030302(R) (2011).
- [16] C. Heussinger and J.-L. Barrat, Phys. Rev. Lett. **102**, 218303 (2009).
- [17] D. Feinstein, M. Van-Hecke, Nature **425**, 256 (2003).
- [18] D. Feinstein, J.W. van-de-Meent and M. Van-Hecke, Phys. Rev. Lett. **92**, 094301, (2004).
- [19] V. Chikkadi, G. Wegdam, D. Bonn, B. Nienhuis, and P. Schall, Phys. Rev. Lett. **107**, 198303 (2011).
- [20] A W Lees and S F Edwards 1972 J. Phys. C: Solid State Phys. **5** (1972).
- [21] C.S. O'Hern, L.E. Silbert, A.J. Liu, and S.R. Nagel, Phys. Rev. E **68**, 011306 (2003).
- [22] J.A. Drocco, M.B. Hastings, C.J. Olson Reichhardt, and C. Reichhardt, Phys. Rev. Lett. **95**, 088001 (2005).